Protoplasma (1995) 189: 238–248

PROTOPLASMA

Ultrastructural analysis of cell component distribution in the apical cell of *Ceratodon* protonemata

L. M. Walker* and **F. D. Sack**

Department of Plant Biology, The Ohio State University, Columbus, Ohio

Received November 7, 1994
Accepted June 12, 1995

Summary. A distinctive feature of tip-growing plant cells is that cell components are distributed differentially along the length of the cell, although most ultrastructural analyses have been qualitative. The longitudinal distribution of cell components was studied both qualitatively and quantitatively in the apical cell of dark-grown protonemata of the moss *Ceratodon*. The first 35 µm of the apical cell was analyzed stereologically using transmission electron microscopy. There were four types of distributions along the cell's axis, three of them differential: (1) tubular endoplasmic reticulum was evenly distributed, (2) cisternal endoplasmic reticulum and Golgi vesicles were distributed in a tip-to-base gradient, (3) plastids, vacuoles, and Golgi stacks were enriched in specific areas, although the locations of the enrichments varied, and (4) mitochondria were excluded in the tip-most 5 µm and evenly distributed throughout the remaining 30 µm. This study provides one of the most comprehensive quantitative, ultrastructural analyses of the distribution of cell components in the apex of any tip-growing plant cell. The finding that almost every component had its own spatial arrangement demonstrates the complexity of the organization and regulation of the distribution of components in tip-growing cells.

Keywords: Tip growth; Stereology; Protonemata; Moss; *Ceratodon*.

Abbreviations: CER cisternal endoplasmic reticulum; ER endoplasmic reticulum; N_d numerical density; SE standard error; S_v surface density; TEM transmission electron microscopy; TER tubular endoplasmic reticulum; V_v volume fraction.

Introduction

The growth of moss protonemata is polarized since extension is restricted to the apical region of the tip cell (Schnepf 1986). In contrast to most other tip-growing cells, such as pollen tubes and root hairs, the protonemal apical cells of several mosses orient their growth according to the direction of gravity and light (Cove et al. 1978, Hartmann et al. 1983, Jenkins et al. 1986, Walker and Sack 1990). Therefore, moss protonemata are a useful system in which to study not only straight tip-growth, but also the directional control of the growth process, since the direction of growth can easily be manipulated by changing the direction of environmental cues.

Tip-growth is associated with an intrinsic cell polarity characterized by gradients in the distribution of cell components (Sievers and Schnepf 1987, Steer and Steer 1989), a polar distribution of calcium (Reiss et al. 1983, Hartmann and Weber 1988) and a differential spatial pattern of ionic currents (Harold and Caldwell 1990). Despite interest in tip-growing cells, a comprehensive, stereological analysis of the distribution of all membrane-bound components within any tip-growing cell has never been reported. Although the distribution of organelles has been studied, analyses have been primarily qualitative (Schmiedel and Schnepf 1980, Grove et al. 1970, Steer and Steer 1989).

In these qualitative studies, some or all cell components have been described as being distributed differentially along the length of the cell. Although generalizations about distributions of cell components for all tip-growing cells have been suggested (Schnepf 1986, Sievers and Schnepf 1987), there are differences between taxa and types of tip-growing cells. Most tip-growing cells appear to contain three broad zones, the apical, subapical, and vacuolar regions. But variation exists in the lengths of zones, the number and types of

* Correspondence and reprints: Department of Biology, 142 Jordan Hall, Indiana University, Bloomington, IN 47405, U.S.A.

organelles found in those zones, and in the distributions of components along the length of the cell (Schmiedel and Schnepf 1980, Steer and Steer 1989, Grove et al. 1970, Bartnik and Sievers 1988). It is not clear how much the variation that has been reported is due to the lack of quantification or to inherent differences between cell types.

The zonation of plastids and microtubules in apical cells of dark-grown protonemata of the moss *Ceratodon* have previously been described based on light microscopy (Walker and Sack 1990, Schwuchow et al. 1990). Here we used transmission electron microscopy (TEM) and stereological techniques to determine the organization of cell components in vertical protonemata. Dark-grown *Ceratodon* protonemata were studied since they are negatively gravitropic (Walker and Sack 1990, Young and Sack 1992). Thus, a stereological analysis of dark-grown vertical protonemata is not only useful for understanding cell organization relating to straight tip growth, but also provides baseline data for comparison with protonemata that have been turned to the horizontal (gravistimulated 90°). Results of such a stereological analysis relating to gravitropism will be presented elsewhere.

Materials and methods

Plant material and fixation techniques

Maintenance and fixation conditions for stock cultures have been described previously (Walker and Sack 1990, 1991). The following micronutrients were added to all media: 70 µm H_3BO_3, 14 µm $MnCl_2$, 0.5 µm $CuSO_4$, 1 µm $ZnSO_4$, 0.2 µm $NaMoO_4$, 10 µm NaCl, 0.01 µm 10 µm $CoCl_2$. Protonemata were sown approximately 1 mm deep in 2% agar medium and grown with the dish on edge in darkness. In addition, a small opening was made in the plates prior to placement in the dark so fixative could be added without disturbing the protonemata. Growing protonemata in agar maintained the position of the protonemata during fixation and allowed for minimal handling. Following 5 days of growth in the dark, each dish contained hundreds of vertically growing, upright protonemata. These protonemata were chemically fixed (approximately 15 ml of fixative) in position for 1.5 h in complete darkness. Darkness is essential since protonemata are phototropic, gravitropism is inhibited by low energy omnilateral light, and plastid zonation changes upon exposure to light (Hartmann et al. 1983, Young and Sack 1992). The fixative consisted of 2% glutaraldehyde, 1% (w/v) paraformaldehyde, 50 mM sodium cacodylate, and 5 mM $CaCl_2$ (pH 6.8). Protonemata (still in agar) were rinsed in buffer, post-fixed in 1% osmium tetroxide (1 h), dehydrated in an acetone series, and then infiltrated with Spurr's epoxy resin (8–12 h). Serial longitudinal sections were cut with a diamond knife, picked up with formvar-coated metal loops (5 mm diam.), placed on slot grids (1 mm × 2 mm), and stained with lead citrate and uranyl acetate. Serial sectioning of protonemata ensured that true median sections were used in the analysis. A Zeiss 10C transmission electron microscope was used to view sections at 60–80 kV.

Sampling

A montage of micrographs from a single median longitudinal section from each vertical protonema was used for the analysis of cell components. The micrographs had a total magnification of × 32,000. Stereological analysis was limited to the apical 35 µm of the cell which was divided up into 5 µm intervals. Nine vertical protonemata were evaluated stereologically.

The distributions of cisternal endoplasmic reticulum (CER), tubular endoplasmic reticulum (TER), Golgi stacks, Golgi vesicles, mitochondria, plastids, and vacuoles were analyzed stereologically with respect to either surface density, S_v, or volume fraction, V_v. Numerical density, N_d, was also calculated for Golgi vesicles.

Calculation of surface density

Surface density, S_v, was calculated for CER and TER. A 1 cm multipurpose test system (Merz 1967) was employed to eliminate an over- or underestimation of anisotropic structures such as ER (Weibel 1989). Surface densities were determined for each 5 µm interval of each apical cell according to standard formulas for the Merz grid (Weibel 1989). Briefly, surface density was calculated from the equation

$$S_v = (2 \cdot I) / (TL \cdot MC),$$

where I is the number of intersections of a "unit membrane" with the lines on the Merz grid, TL is the total grid line length falling over cytoplasm, and MC is a magnification correction so that line length is expressed in micrometer. Since tangentially sectioned membranes can also lead to an overestimation of surface density, tangentially sectioned membranes that crossed each test line were counted as one rather than two intersects (Steer 1981). CER and TER were scored concurrently to avoid counting membrane that was transitional between CER and TER more than once. The cytoplasm was defined operationally as the cell (protoplast) minus plastids and vacuoles (the nucleus is never present within the tipmost 35 µm of the apical cell). Total line length was determined using the equation for the Merz grid,

$$TL = Pt \cdot (\pi/2) \cdot d,$$

where Pt is the number of points falling over cytoplasm and d is the distance (in cm) between the test points on the Merz grid. The Merz grid was placed randomly over the 5 µm interval being sampled.

Calculation of volume fraction

The 1 cm Merz grid is a multipurpose test grid and was also used to calculate the volume fraction of plastids, vacuoles and the area of the cytoplasm in the interval being sampled. A 7 mm square point grid was used to calculate the volume fraction of Golgi stacks, Golgi vesicles, and mitochondria. A Golgi stack was operationally defined as having at least two cisternae visible in a section normal to the stack of cisternae, or a system of anastomosing tubules with budding and/or fusing vesicles attached (sectioned in the major plane of a cisternum). Vesicles were counted as discrete entities if no attachment to the Golgi occurred in that single plane of section. Golgi stacks and vesicles were counted concurrently to eliminate the need to determine whether or not a vesicle was part of the Golgi stack more than once.

Volume fractions, V_v, were determined for each cell interval and calculated from both the 7 mm square dot grid and the 1 cm Merz grid

according to Weibel (1989). Volume fraction was calculated from the equation

$V_v = Pt_x / Pt_c$,

where Pt_x is the number of points on the cell component and Pt_c is the total number of points falling over cytoplasm in the interval. All grids were placed randomly over the micrograph of the interval being sampled.

The cell points counted using the 7 mm square point grid were 700–1,500 points per interval and 7,000–10,000 points per protonema. The cell point count for the 1 cm multipurpose Merz grid was 400–800 points per interval and 3,300–4,500 points per protonema. The total point count was >75,000 and >37,000 for each protonema using the 7 mm and 1 cm grid, respectively. The level of counting resulted in a counting error of no more than 1.4–2.8% for all cell components analyzed.

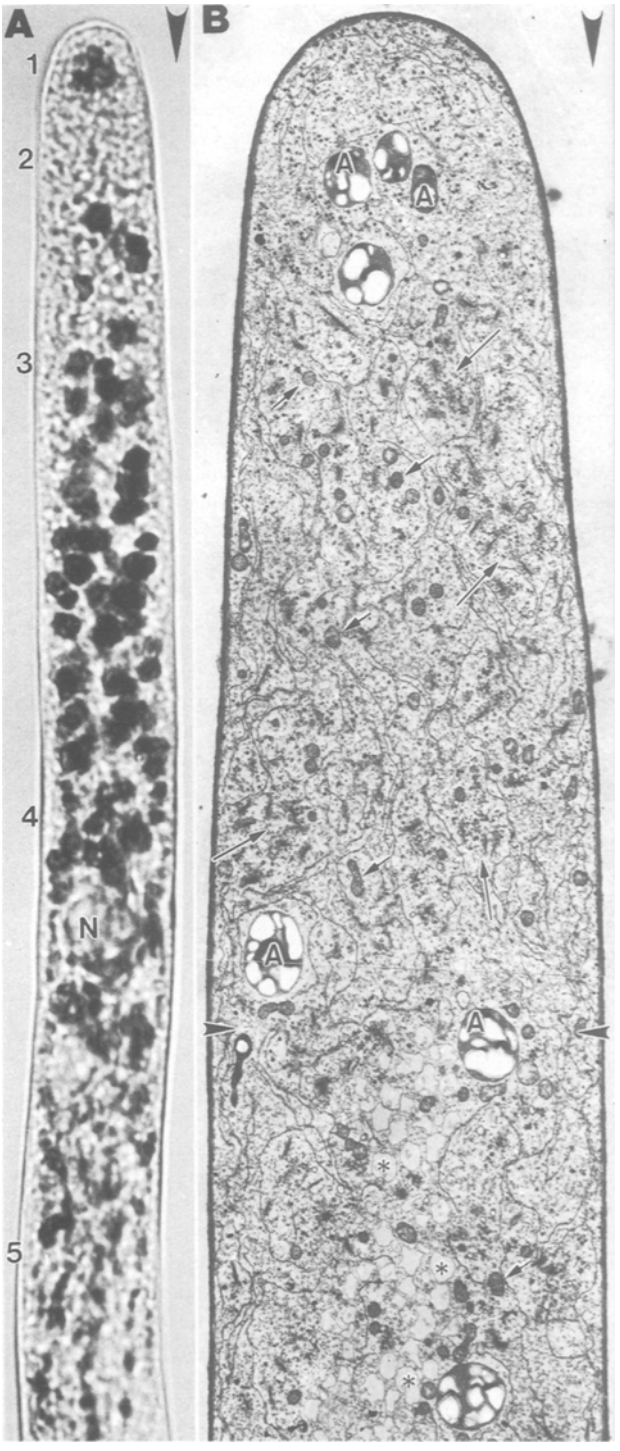

Calculation of numerical density

Vesicles were analyzed with respect to numerical density as well as volume fraction. Five of the nine protonemata were chosen randomly from the overall sample to calculate the number of vesicles per cubic micrometer of cytoplasm, N_d. The Saltykov method for determining sphere density was employed (Steer 1981) and the analysis used four size classes of vesicles.

Statistics

To detect differences in the distribution of cell components along the length of the cell within vertical protonemata, a mixed model, two-way analysis of variance (without replication and utilizing protonema as a random blocking factor), was used to detect statistical differences ($P \leq 0.05$) in the surface density or volume fraction of cell component among all intervals.

Since all data were determined to have a normal distribution, including data collected as a proportion, the original untransformed data were employed in the analysis (Zar 1984). The Tukey test was employed as the multiple comparison test. All statistics were performed using the computer program SAS (SAS Institute 1985).

Results

Qualitative description of distributions in the entire apical cell

Dark-grown *Ceratodon* protonemata have a distinct zonation of amyloplasts in the apical cell with respect both to distribution along the cell length and gravity (Walker and Sack 1990, Schwuchow and Sack 1993). These zones include (1) non-sedimenting amyloplasts in the apex, (2) an amyloplast-free zone, (3) a zone with pronounced amyloplast sedimentation, (4) a zone with mostly non-sedimenting amyloplasts, and

Fig. 1. A Light micrograph of upright (negatively gravitropic) dark-grown *Ceratodon* apical cell. Plastid zones are numbered (*1–5*). Cell was fixed in position, stained with IK_2I, and examined intact with bright field optics. Arrowhead indicated direction of gravity vector. *N* Nucleus. × 1,100. **B** Electron micrograph of median longitudinal section of dark-grown apical cell of *Ceratodon* protonema. This region includes plastid zones 1, 2, and the beginning of zone 3. The apical 35 µm area was analyzed stereologically and is delimited by the arrowheads. Note the abundant cisternal endoplasmic reticulum in plastid zones 1 and 2. The large vesicles (asterisks) were presumably derived from the fixation-induced breakup of vacuolar channels that extend through plastid zone 3. Note the tapering of the tip of the apical cell presumably due to the presence of radial growth behind the apical dome. Long arrows, clusters of Golgi stacks; short arrows, mitochondria; arrowhead, direction of gravity vector; *A* amyloplast. × 4,400

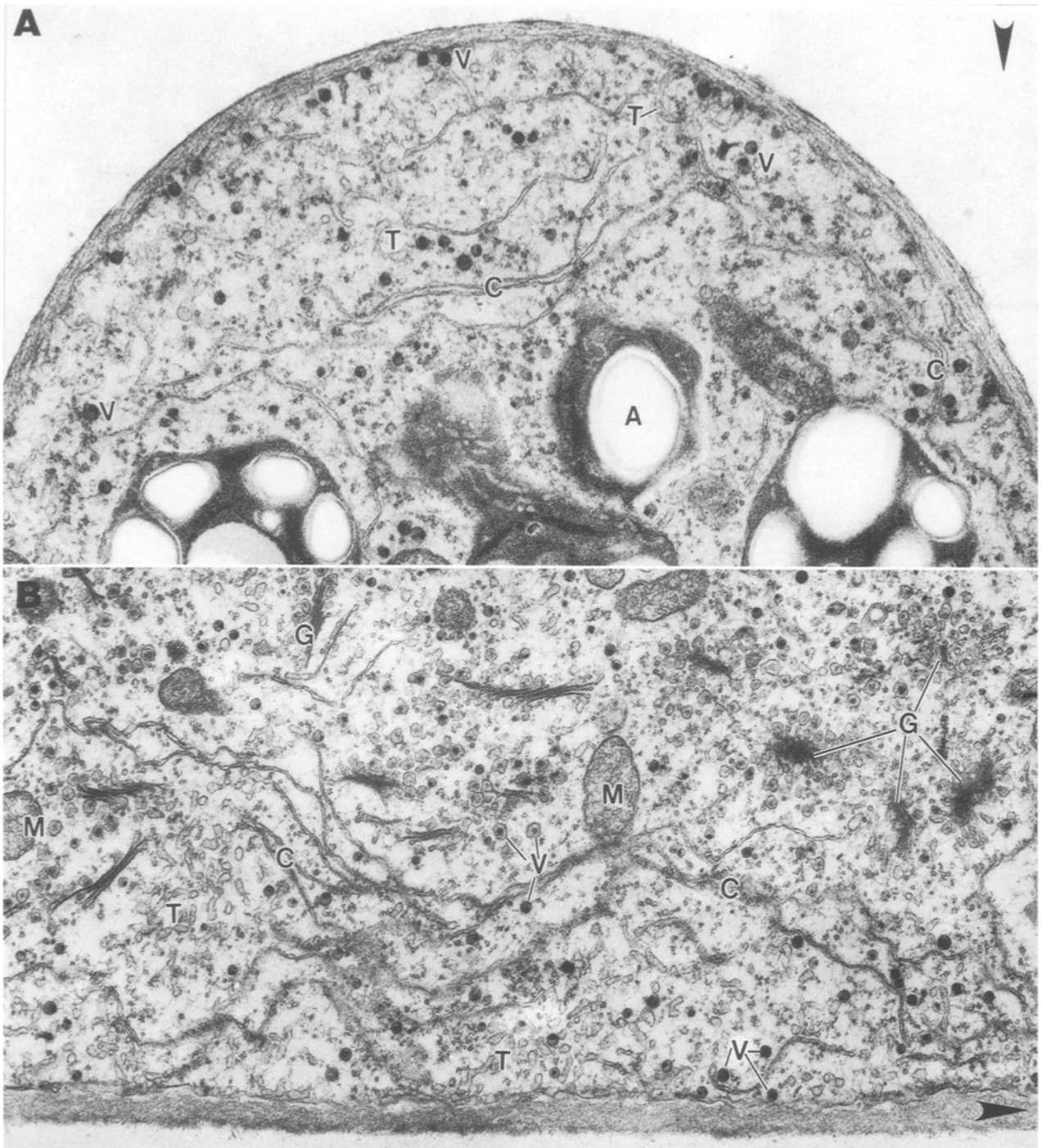

Fig. 2. A Longitudinal section through part of the apical dome. Note the electron dense Golgi vesicles (*V*), cisternal ER (*C*), tubular ER (*T*), and amyloplasts (*A*). Arrowhead, direction of gravity vector. × 22,000 **B** Longitudinal section through the plastid-free zone (zone 2) demonstrating the high density of Golgi stacks (*G*). Note the tubular ER (*T*), the electron dense Golgi vesicles (*V*), and mitochondria (*M*). *C* Cisternal ER. Arrowhead, direction of gravity vector. × 16,200

(5) a vacuolar zone with non-sedimenting amyloplasts (Fig. 1 A).

The nucleus occurred in plastid zone 4 and maintained a distance of approximately 120–150 µm from the tip. The distance of the nucleus from the tip varied with the cell cycle and was closest to the tip after cell division.

Cisternal endoplasmic reticulum (CER) was present

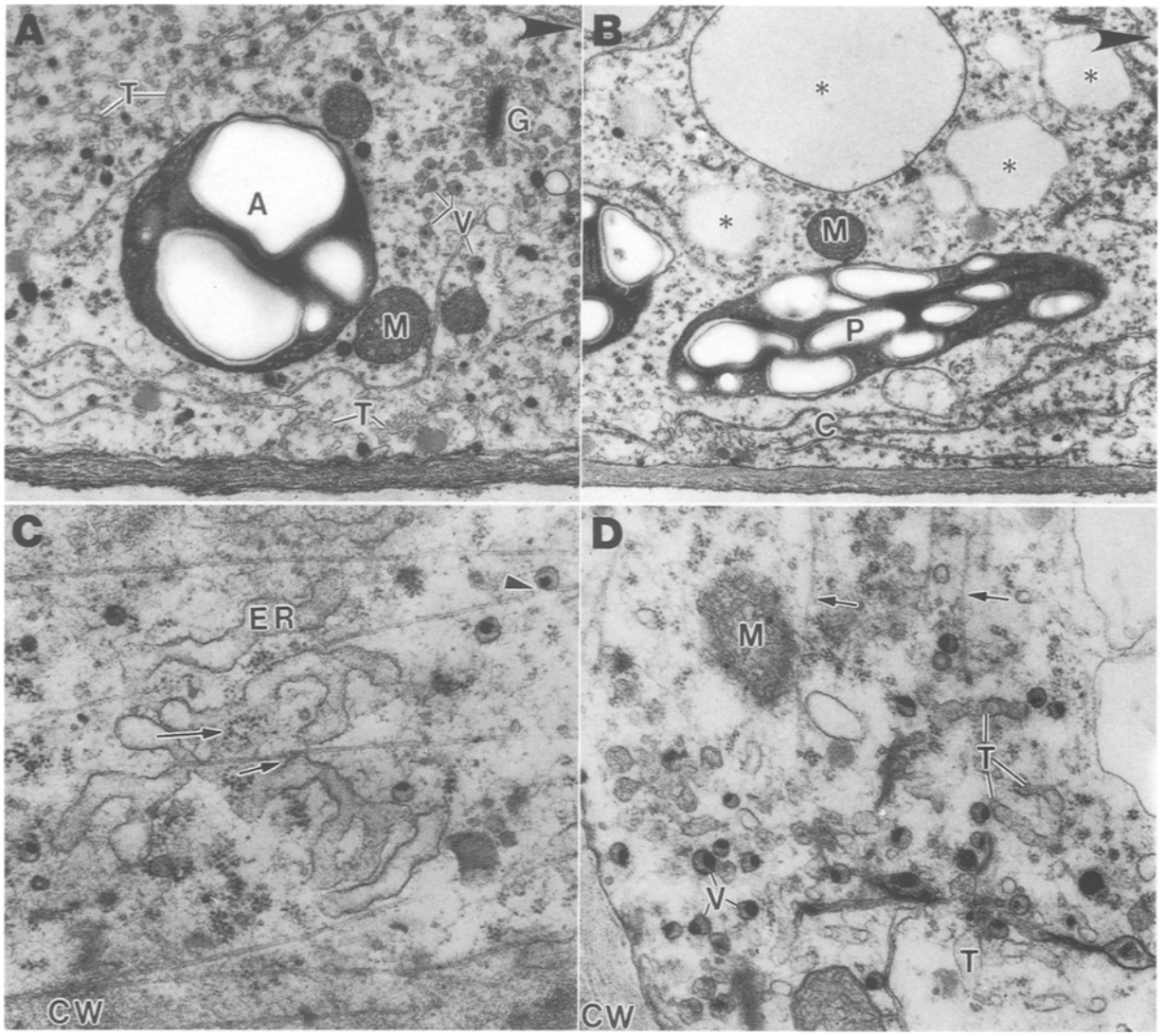

Fig. 3. A Spherical amyloplast (*A*) near apex (plastid zone 1). Note the proximity of plastids and mitochondria (*M*). *V* Golgi vesicles, *G* Golgi stack, *T* tubular ER. Arrowhead, direction of gravity vector. × 14,200. **B** Elongated amyloplast (*P*) in plastid zone 4. The cisternal ER (*C*) is primarily peripheral and parallel to the length of the cell. The tubular ER and electron dense Golgi vesicles are not as abundant in this region as they are in regions closer to the apex (compare with Fig. 2 A, B). Asterisks, vacuoles; *M* mitochondria; arrowhead, direction of gravity vector. × 11,100. **C** Glancing section through cell wall (*CW*), plasma membrane and cytoplasm in the plastid-free zone (zone 2). Some of the cortical ER (*ER*) is associated with polyribosomes (long arrow) and microtubules (short arrow). Microtubules are also close to electron dense Golgi vesicles (arrowhead). × 41,200. **D** Longitudinal section of cell through developing cell plate. Note the numerous electron dense Golgi vesicles (*V*), tubular ER (*T*), and microtubules (arrows). *M* Mitochondria, *CW* cell wall. × 28,100

throughout plastid zones 1 and 2 (Figs. 1 B and 2 A, B). In zones 3–5 CER was mostly located along the side walls and was more longitudinally oriented than in plastid zones 1 and 2 (Figs. 1 B and 3 A, B). Tubular endoplasmic reticulum (TER) was present throughout all 5 plastid zones, and in contrast to CER, was not preferentially located along the side walls in plastid zones 3–5 nor was TER mostly oriented along the long axis of the cell. The tubular and cisternal endoplasmic reticulum and the Golgi vesicles appeared to be more abundant in the first several micrometers of the apex than in the rest of the cell (compare Fig. 2 A to Fig. 3 A, B).

Golgi stacks appeared most abundant in the first 60 µm of the apical cell, but were excluded from the first few micrometers of the apex (Fig. 2 A). Mitochondria were excluded from the apical 5 µm and appeared to be distributed evenly throughout the rest

of the cell (Fig. 1 B). Golgi stacks were not oriented preferentially with respect to any axis of the cell (Fig. 1 B). Lipid bodies were present, but usually occurred in the basal regions of the cell, and were seldom observed within the apical 40 µm of the cell.

Vacuolation began 30–40 µm behind the apex in the amyloplast sedimentation zone (Fig. 1 B). Discrete vacuolar channels were present in the amyloplast sedimentation zone in living cells (Young and Sack 1992), but in fixed cells these channels appeared to have vesiculated. The area occupied by vacuole increased with increasing distance from the tip of the cell.

Morphology of components in entire apical cell

All plastids had large amounts of starch present and thus are considered amyloplasts. Each amyloplast had 2–5 thylakoids in each section. The amyloplasts were more spherical in plastid zones 1 and 3 than amyloplasts in the basal regions of the cell (plastid zones 4 and 5) where plastids were more elongated (Fig. 3 A, B). Amyloplasts in different zones were distended with starch regardless of position. In longitudinal sections of the apical cell, the mitochondria exhibited circular profiles throughout the tip and more elongated profiles in the basal portions of the cell.

The number of Golgi cisternae in a stack appeared to vary slightly from the tip to the base of the cell. Between the apex and the beginning of the amyloplast sedimentation zone (the apical 30 µm or intervals 1–6) the average number of Golgi cisternae in a stack was 3.7 ± 0.06 (SE, N = 915). From the beginning of the amyloplast sedimentation zone to the nucleus the average number of the Golgi cisternae was 3.2 ± 0.07 (N = 643), and from the nucleus to the end wall the number of cisternae in a stack was 3.0 ± 0.13 (N = 303). Golgi cisternae appeared more elongated in the basal region of the cell compared to the apical region. Also the number of vesicles around the Golgi stacks appeared to decrease as the distance from the tip of the cell increased. Vesicles were 60–180 nm in diameter. Within the apical 35 µm, these vesicles consistently had an electron dense core regardless of whether they were close to the Golgi stack or the plasma membrane (Figs. 1 B–3 D). Beyond the apical 35 µm, vesicles were not as electron dense.

The cell wall was fairly uniform in thickness throughout the apical cell and did not appear thinner at the tip of the apical cell where growth was taking place. Although cell wall thickness did not vary within an apical cell, it did vary between apical cells. The cell wall appeared fibrillar without layers or any obvious differences in substructure along the length of the cell.

Apical cells had polygonal networks of cortical endoplasmic reticulum. Microtubules were closely associated with the cortical endoplasmic reticulum, vesicles (Fig. 3 C), and with plastids. There was also a close positional association between some mitochondria and plastids (Fig. 3 A, B). Numerous plasmodesmata were present in the end wall. No microfilaments were seen in the TEM.

Stereological description of distribution of cell components within the apical 35 µm

Since dark-grown apical cells of *Ceratodon* protonemata range in size from about 150 µm (postmitotic) to 400 µm (premitotic) in length, the 35 µm analyzed includes 9–23% of the entire cell length. As with other tip-growing cells, vacuolar area is proportional to cell length. In *Ceratodon*, preliminary evidence indicates that cell extension occurs in the apical 10 µm of the cell (Schwuchow 1991). In addition to extension, careful serial sectioning of *Ceratodon* revealed a taper to the apex (Fig. 1 B), suggesting that radial growth occurs behind the apex. Thus, the region analyzed stereologically included the zone of growth, the expanding region behind the dome, and regions that were nongrowing (Fig. 1 B).

Stereological (morphometric) analysis demonstrated that most cell components within the first 35 µm of the apical cell of *Ceratodon* were distributed differen-

Table 1. Effect of interval on cell component distribution, mixed model, two-factor analysis of variance (without replication and using protonema as a random blocking factor)

Cell	P
Cisternal ER	0.0001
Tubular ER	0.5700
Golgi stacks	0.0001
Golgi	0.0001
Mitochondria	0.0007
Plastids	0.0001
Vacuole	0.0001

All cell components, except the tubular endoplasmic reticulum, had test significance values of $P \leq 0.001$. Thus, these cell components had statistically significant differences in abundance among some intervals, indicating a non-uniform distribution

P Probability

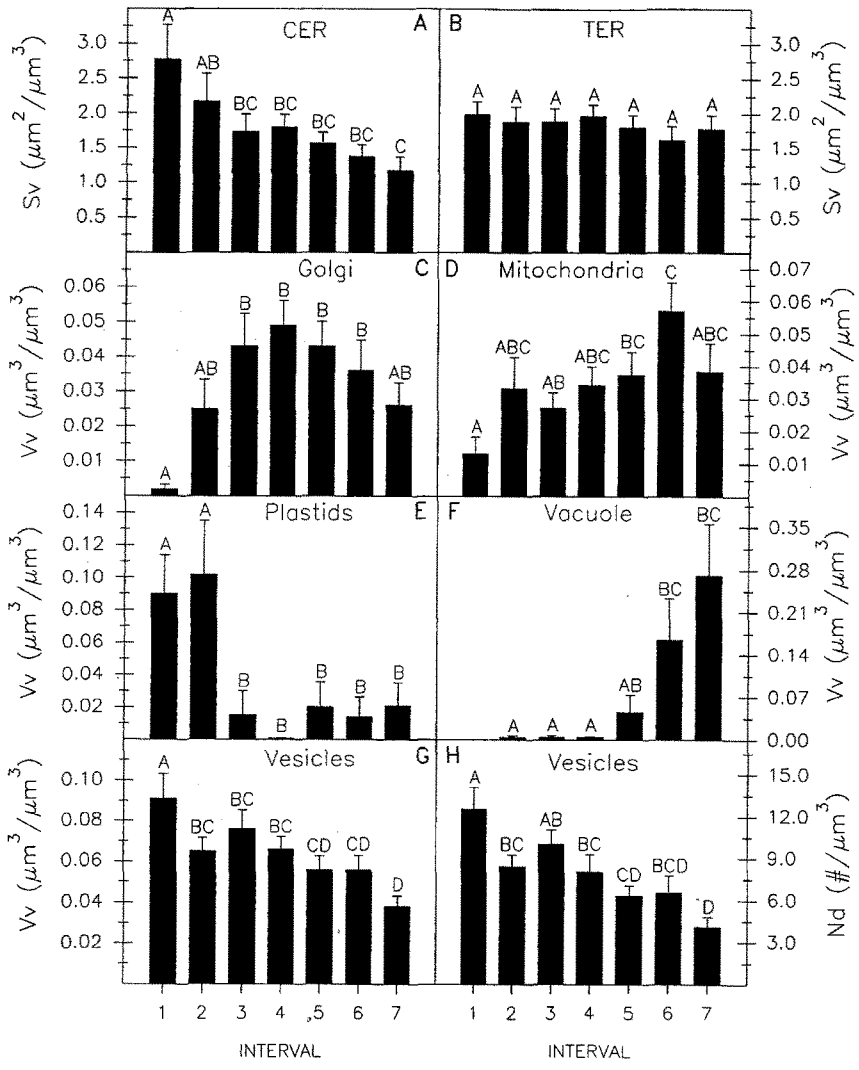

Fig. 4. Histograms demonstrating surface density, S_v (**A** and **B**), and volume fraction, V_v (**C–G**), of cell components as a function of distance from the tip in dark-grown *Ceratodon* protonemata. Vesicles were also evaluated with respect to numerical density, N_d (**H**). Each interval represents a 5 μm distance. Interval 1 includes the apical dome and interval 7 is closest to the base of the cell. Within each individual histogram, intervals that share the same letter (*A–D*) are not statistically different. Standard error bars are indicated. Note that different cell components have different distributions. *CER* Cisternal and *TER* tubular endoplasmic reticulum

tially along the length of this region. The only exception was the tubular endoplasmic reticulum (Table 1). The distributions of cell components in the first 35 μm fell into four types or categories: (1) an even distribution, (2) a tip-to-base gradient, (3) an enrichment in specific intervals, and (4) an exclusion of cell components in interval 1 and an even distribution throughout the other intervals.

Even distribution

The TER was the only cell component that was evenly distributed in the first 35 μm. There were no significant statistical differences between any of the seven intervals when all protonemata were analyzed as a sample (Table 1). The mean surface density of TER in the entire region analyzed (all seven intervals) was 1.84 μm^2 of membrane surface/μm^3 cytoplasm. In addition, none of the individual protonemata exhibited a differential distribution in TER within the area analyzed (Fig. 4 B).

Tip-to-base gradient

Cisternal endoplasmic reticulum (CER) and Golgi vesicles both exhibited a tip-to-base gradient in their distribution in the 35 μm region analyzed. Thus, CER and vesicles were most abundant in the first intervals and the least abundant in the most basal intervals.

CER: The pattern of differences in the surface density between some intervals suggests the presence of a tip-to-base gradient of CER (Fig. 4 A). Interval 1 was statistically different from intervals 3–7. Intervals 1 and 2 had the largest surface densities, which were statistically different from interval 7, which had the lowest surface density. Although surface density appears to decrease from intervals 2 to 6, these values were not statistically different from each other. Indi-

vidually, six of the nine vertical protonemata each had distinct tip to base gradients in CER, while a seventh had a weak tip to base gradient. The other two protonemata had no obvious CER gradients, but even in these protonemata, the lowest surface density values were in interval 7.

Vesicles: Golgi vesicles (indentified by the presence of electron dense contents) in the apical 35 µm appeared to be distributed in a tip-to-base gradient as indicated both by vesicle volume fraction and numerical density (Fig. 4 G, H). For volume fraction, interval 1 was statistically different from all intervals and intervals 1–4 were statistically different from interval 7, more or less indicating the presence of a tip-to-base gradient. Interval 1 had a volume fraction of 0.091 $\mu m^3/\mu m^3$, while interval 7 had a volume fraction of 0.038 $\mu m^3/\mu m^3$.

Analysis of individual protonemata showed a tip-to-base gradient in each of eight of the nine protonemata sampled. The presence of a tip-to-base gradient from 0–35 µm was confirmed by determining the vesicle numerical density for five protonemata (Fig. 4 H).

Enrichment of cell components in specific intervals

The Golgi stacks, plastids and vacuole fit into this type of distribution although their individual distributions varied from each other.

Golgi stacks: There was a statistically significant difference in the volume fraction of Golgi stacks between some of the intervals in vertical protonemata (Fig. 4 C). Intervals 1, 2, and 7 contained the lowest volume fractions. Interval 1 was statistically equivalent to intervals 2 and 7 but statistically different from intervals 3–6. When the statistical post-test conditions were relaxed (Duncan rather than a Tukey post-test), intervals 3–5 become statistically different ($P \leq 0.05$) from all other intervals (data not shown), indicating an enrichment of Golgi stacks in intervals 3–5. Individually, each of seven of the nine protonemata had an obvious enrichment of Golgi stacks in intervals 3–5 (30–40% increase in V_v) as compared to intervals 2 and 7. No comparison (based on percent increase) between interval 1 and other intervals could be made, since most apical cells had no Golgi stacks ($V_v = 0$) in interval 1. The area of enrichment in individual protonemata was variable (Table 2), and this variability appeared to mask the presence of an enrichment when data from all of the protonemata were subjected to a Tukey post-test (Fig. 4 C).

Plastids: Intervals 1 and 2 were statistically different from all other intervals (Fig. 4 E). The presence of plastids in the very tip and their almost complete absence from intervals 3–7 has been reported previously and confirms that the first 35 µm includes plastid zones 1 and 2 (Walker and Sack 1990, Young and Sack 1992).

Vacuole: The volume fraction of vacuole was calculated from the total protoplasmic volume. Interval 7 was statistically different from all intervals except interval 6 (Fig. 4 F). No vacuole was present in interval 1 and interval 7 had the largest volume fraction.

Table 2. Distribution (by interval) of volume fraction of Golgi stacks in three different representative protonemata

	Interval						
Cell		1	2	3	4	5	6, 7
1	0.01	0.02	0.04	0.07	0.05	0.02	0.0
2	0.00	0.01	0.01	0.04	0.04	0.04	0.0
3	0.00	0.04	0.02	0.06	0.03	0.00	0.0

Note that the specific position of the enrichment varies from cell to cell. Values are in μm^3 of Golgi cisternae/μm^3 of cytoplasm (S_v)

Exclusion of cell complements in the very tip and an even distribution elsewhere

Mitochondria: Only the mitochondria fit into this category. Mitochondria were largely absent from the first 5 µm (Fig. 4 D). Although the average volume fraction in the first interval was 0.013 $\mu m^3/\mu m^3$, all mitochondria which were present in interval 1 were observed 4–5 µm from the tip and mitochondria were excluded from the first 3 µm of the tip. Individually, six of the nine protonemata had a very strong exclusion of mitochondria from their first 5 µm. Mitochondria present in intervals 2–7 were more or less evenly distributed, although it is possible that mitochondrial volume fraction increases towards the base of the region analyzed (intervals 5–7).

Discussion

This study provides the most comprehensive, ultrastructural analysis of the distribution of cell components in the apex of any tip-growing plant cell and reveals many intriguing features of cell organization. Other ultrastructural analyses of tip-growing cells have been qualitative (Schmiedel and Schnepf 1980, Sievers 1967) or have used stereology to analyze the distribution of only one or two cell components

(Kwon et al. 1991; Picton and Steer 1981, 1983; Jensen and Jensen 1984). This study, which is the first stereological analysis of the distribution of the endoplasmic reticulum for any tip-growing plant cell, demonstrates that the CER and the TER are distributed differently but that the greatest abundance of total ER occurs in the most apical part of the cell.

Generalizations about distributions in all tip-growing cells

Ultrastructural studies indicate that different tip-growing cells, such as pollen tubes, fungal hyphae, moss and fern protonemata, algal rhizoids and root hairs, all share some common features. Studies to date suggest that tip-growing cells have three basic zones, the apical, subapical, and vacuolar zones.

The apical region is where growth is localized and where large organelles such as mitochondria, plastids, nuclei, lipid bodies, and vacuoles generally seem to be excluded (Steer and Steer 1989, Heath and Kaminskyj 1989, Sievers and Schnepf 1987). The apical region contains numerous vesicles (Steer and Steer 1989, Schmiedel and Schnepf 1980, Heath et al. 1985, Sievers et al. 1979) and ER of varying morphologies (Sievers and Schnepf 1987, Bartnik and Sievers 1988, Jensen and Jensen 1984, Wada and O'Brien 1975).

The subapical region is characterized by the presence of numerous components such as mitochondria, Golgi, plastids, rough and smooth ER, and nuclei. Qualitative observations suggest that these organelles decrease in abundance in the vacuolar region which is basipetal to the subapical region (Cresti et al. 1977, 1985; Grove et al. 1970; Schmiedel and Schnepf 1980). However, the rough ER in *Physcomitrium* and the mitochondria in *Neurospora* are reported to be evenly distributed (Jensen and Jensen 1984, Zalokar 1959).

Component distribution in Ceratodon apical cells

The different distributions of cell components along the length of the apical cell in *Ceratodon* emphasize the complexity of cell organization. With the exception of the tubular endoplasmic reticulum (TER), all cell components analyzed were differentially distributed within the first 35 µm of the cell. The cisternal endoplasmic reticulum (CER) and Golgi vesicles were distributed in a tip-to-base gradient. The plastids, vacuole and Golgi stacks all had specific areas of enrichment, although individual distributions varied from each other. The mitochondria were excluded from the first several micrometers of the tip but were evenly distributed along the rest of the region analyzed. Thus, almost every cell component has a different distribution.

Differential distributions of cell components in tip-growing cells are presumably adaptive for tip-growth, although few data exist regarding the function of zonation. It is presumed that components in the apical dome, such as ER and vesicles, are most immediately involved in extension. For example, Golgi vesicles must be supplying exocytotic products involved in wall formation and membrane necessary for the growth of the plasma membrane.

The functional significance of the abundance of ER in the dome is not known, but it is plausible that it regulates calcium levels in the cytosol. In plant cells, calcium is thought to be stored within the ER (Hepler et al. 1990) and the calcium concentration affects tip growth (Picton and Steer 1982, Kropf and Quatrano 1987, Miller et al. 1992).

Although their products are clearly essential for growth, other cell components such as Golgi stacks and mitochondria are mostly absent from the apical dome. Thus, it is surprising that plastids are present so close to the apex in *Ceratodon*, since they are presumably not directly involved in tip extension, and their relative size would appear to interfere with vesicle movement and deposition in the apex. These tip plastids might be involved in gravitropic sensing for the initial downward curvature in gravistimulated protonemata (Walker and Sack 1991).

Comparison of moss protonemata with other tip-growing cells

Both qualitative (*Funaria*), and stereological (*Ceratodon*) studies of Golgi stacks in moss protonemata indicate that the greatest density of Golgi stacks occurs 10–25 µm behind the apex, and that the greatest abundance of vesicles occurs apical to these Golgi stacks (this study; Sievers and Schnepf 1980). This enrichment of Golgi stacks behind the apical dome appears to be a common feature of most tip-growing cells (Steer and Steer 1989, Heath and Kaminskyj 1989).

Unlike moss protonemata, many fungal hyphae and pollen tubes possess a very dense accumulation of vesicles in a region several micrometers behind the tip, and vesicles of two obviously different sizes

(Steer and Steer 1989, Bartnicki-Garcia 1990). However, it is possible that *Ceratodon* has two different types of vesicles, based not on size but on staining pattern. Nearly all the vesicles in the first 35 µm had an obvious electron dense core. Vesicles located further back in the cell, either had or lacked electron dense contents. If this difference in staining were due to a difference in the plane of vesicle sectioning, vesicles with less staining should have been as obvious in the first 35 µm as they were basally. The electron dense Golgi vesicles in *Ceratodon* were observed wherever wall formation was occurring, i.e., at the apex and near the cell plate (Fig. 3 D). Thus, electron dense vesicles may contain cell wall matrix materials, whereas vesicles with little electron density may be involved in processes other than cell wall formation.

There are other differences between moss protonemata and other tip-growing cells. In some pollen tubes and fungal hyphae the long axis of mitochondria and the cis–trans axis of Golgi stacks are parallel to the long axis of the cell (Heath and Kaminskyj 1989, Steer and Steer 1989). The absence of this arrangement in mosses may perhaps relate to an absence of cytoplasmic streaming in protonemata (Young and Sack 1992).

Comparisons between Ceratodon and other moss apical cells

Apical cells of moss protonemata appear to contain spherical plastids in the apical regions and more elongated plastids in the basal regions of the cells (Schmiedel and Schnepf 1980, Jensen and Jensen 1984). However, in *Ceratodon* there does not appear to be a decrease in the volume fraction of starch of plastids or any increase in thylakoid number in the basal region of the apical cell as has been described for *Funaria* (Sievers and Schnepf 1987).

In *Ceratodon*, plastids are present in a group approximately 3–10 µm behind the apex, while in *Funaria* caulonemata and *Physcomitrium* protonemata plastids are present starting 10–20 µm behind the tip (Schmiedel and Schnepf 1980, Jensen and Jensen 1984, Tewinkel and Volkmann 1987, Schwuchow et al. 1995). The functional advantage of these different organizations is unclear since they do not correlate with differences in growth rate or the presence or absence of light (Young and Sack 1992, Jensen and Jensen 1984, Schmiedel and Schnepf 1980, DeMaggio and Stetler 1977).

Growth localization and polarity of tip-growing cells

Analysis of the literature is consistent with the generalization that tip-growing cells with faster growth rates and with more highly localized sites of growth have a more pronounced polarity in the distribution of cell components (Jensen and Jensen 1984, Schmiedel and Schnepf 1980). For example, in very slow growing moss protonemata there is little or no differential distribution of components and large organelles are present in the apex (Schmiedel and Schnepf 1980, DeMaggio and Stetler 1977 and references therein). This lack of longitudinal stratification may be related to the occurrence of extension in areas other than the extreme tip.

Conversely, fast growing pollen tubes, algal rhizoids and moss protonemata have a pronounced cell component polarity which often excludes large organelles from the apex (Heath and Kaminskyj 1989, Bartnik and Sievers 1988, Schmiedel and Schnepf 1980).

Control of the distribution of cell components

The finding that almost every cell component has its own type of distribution in *Ceratodon* protonemata demonstrates how complicated the control and maintenance of polarity is in tip-growing cells. For example, plastids in *Ceratodon* protonemata move considerably yet distinct zones are maintained (Young and Sack 1992). Both microtubules and microfilaments affect plastid position (Schwuchow and Sack 1994), but we do not yet understand how plastid zonation is maintained. In general, little is know about how plant organelles are positioned and this regulation must be particularly intricate in tip-growing cells.

In conclusion, this is the first stereological analysis of a tip-growing plant cell that quantified multiple cell components that included an analysis of the endoplasmic reticulum. It shows that the longitudinal distribution of cell components in *Ceratodon* apical cells is even more complex than has been reported for any other tip-growing cell. Further quantitative analysis of different tip-growing cells should help us understand commonalities and variations in different types of cells as well as assist in understanding how growth is localized to the apex.

Acknowledgements

This work was supported in part by NASA Graduate Student Researchers Program grant (LMW) and by NASA Space Biology grants NAGW-780 and NAG10-0085 (FDS).

References

Bartnicki-Garcia S (1990) Role of vesicles in apical growth and a new mathematical model of hyphal morphogenesis. In: Heath, IB (ed) Tip growth in plant and fungal cells. Academic Press, New York, pp 211–232

Bartnik E, Sievers A (1988) In-vivo observations of a spherical aggregate of endoplasmic reticulum and Golgi vesicles in the tip of fast-growing *Chara* rhizoids. Planta 176: 1–9

Cove DJ, Schild A, Ashton NW, Hartmann E (1978) Genetic and physiological studies of the effect of light on the development of the moss *Physcomitrella patens*. Photochem Photobiol 27: 249–254

Cresti M, Pacini E, Ciampolini F, Sarfatti G (1977) Germination and early tube development in vitro of *Lycopersicon peruvianum* pollen: ultrastructural features. Planta 136: 239–247

– Ciampolini F, Mulcahy LM, Mulcahy G (1985) Ultrastructure of *Nicotiana alata* pollen, its germination and early tube formation. Amer J Bot 72: 719–727

DeMaggio AE, Stetler DA (1977) Protonemal organization and growth in the moss *Dawsonia superba*: ultrastructural characteristics. Amer J Bot 64: 449–454

Grove SN, Bracker CE, Morré DJ (1970) An ultrastructural basis for hyphal tip growth in *Pythium ultimum*. Amer J Bot 57: 245–266

Harold FM, Caldwell JH (1990) Tips and currents: electrobiology of apical growth. In: Heath IB (ed) Tip growth in plant and fungal cells. Academic Press, New York, pp 59–90

Hartmann E, Weber M (1988) Storage of the phytochrome-mediated phototropic stimulus of moss protonemal tip cells. Planta 175: 39–49

– Klingenberg B, Bauer L (1983) Phytochrome-mediated phototropism in protonemata of the moss *Ceratodon purpureus* Brid. Photochem Photobiol 38: 599–603

Heath IB, Kaminskyj GW (1989) The organization of tip-growth-related organelles and microtubules revealed by quantitative analysis of freeze-substituted oomycete hyphae. J Cell Sci 93: 41–52

– Rethoret K, Arsenault AL, Ottensmeyer FP (1985) Improved preservation of the form and contents of wall vesicles and the Golgi apparatus in freeze substituted hyphae of *Saprolegnia*. Protoplasma 128: 81–93

Hepler PK, Palevitz BA, Lancelle SA, McCauley MM, Lichtscheidl I (1990) Cortical endoplasmic reticulum in plants. J Cell Sci 96: 355–373

Jenkins GI, Courtrice GRM, Cove DJ (1986) Gravitropic responses of wild-type and mutant strains of the moss *Physcomitriella patens*. Plant Cell Environ 9: 637–644

Jensen LC, Jensen CG (1984) Fine structure of protonemal apical cells of the moss *Physcomitrium turbinatum*. Protoplasma 122: 1–10

Kropf DL, Quatrano RS (1987) Localization of membrane-associated calcium during development of fucoid algae using chlorotetracycline. Planta 171: 158–170

Kwon YH, Hoch HC, Aist JR (1991) Initiation of appressorium formation in *Uromyces appendiculatus*: organization of the apex, and the responses involving microtubules and apical vesicles. Can J Bot 69: 2560–2573

Merz WA (1967) Die Streckenmessung an gerichteten Strukturen im Mikroskop und ihre Anwendung zur Bestimmung von Oberflächen-Volumen-Relationen im Knochengewebe. Mikroskopie 22: 132–144

Miller DD, Callaham DA, Gross DJ, Hepler PK, (1992) Free Ca^{2+} gradient in growing pollen tubes of *Lilium*. J Cell Sci 101: 7–12

Picton JM, Steer MW (1982) A model for the mechanism of tip extension in pollen tubes. J Theor Biol 98: 15–20

– – (1983) The effect of cycloheximide on dictyosome activity in *Tradescantia* pollen tubes determined using cytochalasin D. Eur J Cell Biol 29: 133–138

Reiss HD, Herth W, Schnepf E (1983) The tip-to-base calcium gradient in pollen tubes of *Lilium longiflorum* measured by proton-induced X-ray emission (PIXE). Protoplasma 115: 153–159

SAS Institute (1985) SAS user's guide: statistics. SAS Institute, Cary, NC

Schmiedel G, Schnepf E (1980) Polarity and growth of caulonema tip cells of the moss *Funaria hygrometrica*. Planta 147: 405–413

Schnepf E (1986) Cellular polarity. Annu Rev Plant Physiol 37: 23–47

Schwuchow J (1991) Untersuchungen zum Gravitropismus und zur Signalverarbeitung in der Protonemaspitzenzelle des Laubmooses *Ceratodon purpureus*. PhD dissertation, Johannes-Gutenberg-Universität, Mainz, Federal Republic of Germany

– Sack FD (1993) Effects of inversion on plastid position and gravitropism in *Ceratodon* protonemata. Can J Bot 71: 1243–1248

– – (1994) Microtubules restrict plastid sedimentation in protonemata of the moss *Ceratodon*. Cell Motil Cytoskeleton 29: 366–374

– Sack FD, Hartmann E (1990) Microtubule distribution in gravitropic protonemata of the moss *Ceratodon*. Protoplasma 159: 60–69

– Kim D, Sack FD (1995) Caulonemal gravitropism and amyloplast sedimentation in the moss *Funaria*. Can J Bot 73: 1029–1035

Sievers A (1967) Elektronenmikroskopische Untersuchungen zur geotropischen Reaktion. Z Pflanzenphysiol 57: 462–473

– Schnepf E (1987) Morphogenesis and polarity of tubular cells with tip growth. In: Kiermayer O (ed) Cytomorphogenesis in plants. Springer, Wien New York, pp 265–299 [Alfert M et al (eds) Cell biology monographs, vol 8]

Steer M (1981) Understanding cell structure. Cambridge University Press, Cambridge

– Steer JM (1989) Pollen tube tip growth. New Phytol 111: 323–358

Tewinkel M, Volkmann D (1987) Observations on dividing plastids in the protonema of the moss *Funaria hygrometrica* Sibth. Planta 172: 309–320

Wada M, O'Brien TP (1975) Observations on the structure of the protonema of *Adiantum capillus-veneris* L. undergoing cell division following white-light irradiation. Planta 126: 213–227

Walker LM, Sack FD (1990) Amyloplasts as possible statoliths in gravitropic protonemata of the moss *Ceratodon purpureus*. Planta 181: 71–77

– – (1991) Recovery of gravitropism after basipetal centrifugation in protonemata of the moss *Ceratodon purpureus*. Can J Bot 69: 1737–1744

Weibel ER (1989) Stereological methods 1: practical methods for biological morphometry. Academic Press, New York

Young JC, Sack FD (1992) Time lapse analysis of gravitropism in *Ceratodon* protonemata. Amer J Bot 79: 1348–1358

Zalokar M (1959) Growth and differentiation of *Neurospora* hyphae. Amer J Bot 46: 602–610

Zar JH (1984) Biostatistical analysis. Prentice-Hall, Englewood Cliffs